[1]Bhaskar Bhookya

[2]B. Mangu

[3] Ravi Bukya

Dual-Sided L-C-C Compensated Wipt Application for Electric Vehicle Battery Charging System

Abstract: This study examines the compatibility of wireless chargers using the dual-sided LCC compensation topology and those using the four fundamental compensation topologies for wireless inductive power transfer systems (WIPT). To provide analysis of dual-sided LCC topology. Main criteria of paper is design considerations for various compensation topologies: (1) secondary sides with series and parallel when using an LCC compensation topology as the primary side; (2) primary sides with series and parallel when using an LCC compensation topology as the secondary side. LCC-S, LCC-P, S-LCC, and P-LCC are four topologies that will be discussed. Verified the analysis with MATLAB/SIMULINK. Even with a 265mm misalignment at 300mm gap, the current-fed DC-DC converter topology has a 95.8% efficiency.

Keywords: Dual sided LCC, Compensation Topologies, Wireless inductive power transfer(WIPT), Electric vehicle(EV), Iinteroperability.

I. INTRODUCTION

Electric vehicles (EVs) and plug-in hybrid electric vehicles (PHEVs) have successfully used inductive power transfer (IPT) wireless chargers[1-2]. The primary and secondary coils form a time-varying electromagnetic field that transfers electrical power. To minimize the power supply's VA rating and increase transferred power, resonant tanks must be constructed with adjustment circuits for both primary and secondary coils. The coupling coefficient for EV and PHEV applications ranges from 0.15 to 0.45, depending on coil size, ground clearance, and misalignment. The load varies with the duration of charging because battery voltage rises during the constant current charging stage and falls during the constant voltage charging stage. Appropriate strategy or methods used to handle these variations. When operating at resonance frequency, both WPT with S-S compensation topology and dual-sided LCC compensation topology have constant output current that is independent of coupling coefficient and load conditions[2-6]. Particularly useful for applications requiring numerous pick-ups, the principal coil current of a dual-sided LCC adjusted wireless charger remains constant, independent of coupling or load[6].

Manufacturers and customers are both concerned about interoperability between different wireless chargers. Concerning interoperable, there are two factors to consider: inter-operability of distinct coil shapes and inter-operability of different compensation topologies[6-9]. Proposes a circular primary pad with spiral square coil and evaluates its interoperability with a square receiver coil and a square receiver coil. Similar square secondary pad is implied in, along with interoperability with circular and square primary pads. These two on other hand, are solely concerned with coil design. In this paper, the interplay between various topologies for primary and secondary sides is addressed. Interactions between the LCC compensated primary side and the parallel compensated secondary side (LCC-P) and series compensated secondary side (LCC-S)[7–8], LCC secondary side (S-LCC) interacting with series compensated primary side, whereas P-LCC secondary side (S-LCC) was interacting with parallel compensated primary side.

II. PROBLEM FORMULATION

*[1]Research Scholar, Dept. of Electrical Engineering, University College of Engineering, Osmania University, Hyderabad, bhaskarouphd@gmail.com
[2]Professor, Dept. of Electrical Engineering, University College of Engineering, Osmania University, Hyderabad bmanguou@gmail.com
[3] Research Scholar, Dept. of Electrical Engineering, University College of Engineering, Osmania University, Hyderabad, raviphd2016@gmail.com

1. Dual-Sided LCC Compensation Topology Analysis

Figure.2.1. [3] shows a dual-sided LCC wireless system links on both primary and secondary sides, an LCC network of inductor-capacitor-capacitor (LCC) is allied to principal coil (L_1 and L_2). Both coils of LCC network tuned at same resonance frequency ω_0. The following equations describe the relationships that should be satisfied by this frequency:

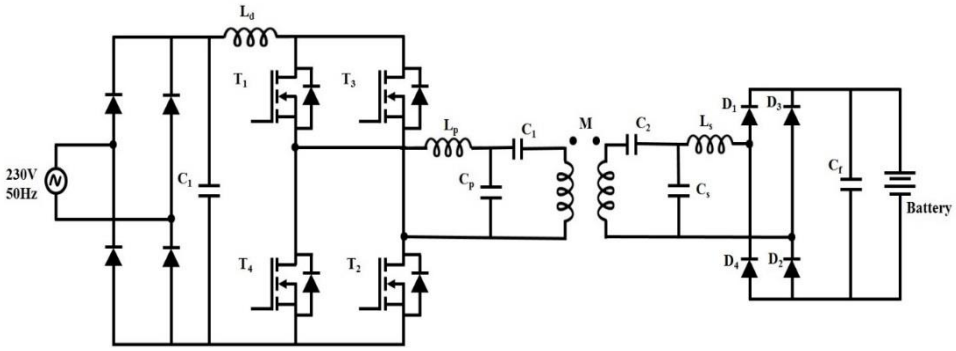

Figure 2.1: Dual-sided LCC compensation topology.

$$\mathrm{mod}\{V_{AB}\} > \mathrm{mod}\{-j\omega_0 M I_2\}$$

$$\omega_o = \frac{1}{\sqrt{L_p.C_p}} = \frac{1}{\sqrt{(L_1 - L_p).C_1}} \quad \text{.....(2.1)}$$

$$= \frac{1}{\sqrt{L_s.C_s}} = \frac{1}{\sqrt{(L_2 - L_s).C_2}} \quad \text{.....(2.2)}$$

If the system is constructed with these assumptions, resonance frequency ω0 will not dependent on coupling coefficient and load circumstances, and will associated be related to L_1, L_p, C_1, C_p, L_2, L_s, C_1, C_s. With the premise that operating angular frequency was zero, following formulas can be determined by first harmonics analysis [10].

$$I_{L_p} = -\frac{k\sqrt{L_1 L_2 V_{ab}}}{j.\omega_o L_p L_s} \quad \text{....(2.3)}$$

$$I_1 = \frac{V_{ab}}{j.\omega_o L_P} \quad \text{.....(2.4)}$$

$$I_2 = -\frac{V_{ab}}{j.\omega_o L_s} \quad \text{.....(2.5)}$$

$$I_{L_s} = \frac{k\sqrt{L_1 L_2 V_{ab}}}{j.\omega_o L_p L_s} \quad \text{.....(2.6)}$$

$$P_{out} = \mathrm{Re}\left(V_{ab} I_{L_s}\right) = \frac{\sqrt{L_1 L_2}}{\omega_o L_p L_s}.kV_{ab}V_{AB} \quad \text{.....(2.7)}$$

where V_{AB} is after inverter output voltage and V_{ab} is input voltage before rectifier, and I_{Ls}* is complex conjugate of I_{Ls}. Shows their connection with input DC voltage V_{in} and voltage of battery V_b:

$$V_{AB} = \frac{1}{\sqrt{2}}\frac{4}{\pi}V_{in}, V_{ab} = \frac{1}{\sqrt{2}}\frac{4}{\pi}V_b \quad \text{.....(2.8)}$$

Current I_1 on primary main coil L_1 is constant, as shown in second item of (2.4), and is only related to input voltage V_{AB}. As indicated in (2.8), relationship between output power and coupling coefficient k, input voltage VAB, and desired output voltage Vab. The following characteristics of dual-sided LCC compensation topology are self-evident:

- Resonant frequency is fixed. Wireless charging system operate at constant frequency regardless coupling coefficient or load.
- Output current is independent of the load.
- The primary main coil has a constant current. Primary coil is transferring power to multiple secondary coils concurrently, this is critical.
- Power factor of primary and secondary sides, nearly unit power factors are accomplished across entire range of operation conditions. As a result, high efficiency attained[12].
- Output power is proportional to the coupling voltage.

2. Inter-Operability Considerations

I. For wireless charging in EVs/PHEVs, the dual-side LCC topology is a better preference. Characteristics such as those listed above are desirable. The reference wireless charging system in this chapter is a dual-sided LCC compensated wireless charger.
Dual-sided LCC topology's parameters are shown in Table I:

Specifications	**Values**
DC Input voltage	<430V
battery voltage	330V~480V
Nominal gap	300 mm
Coefficient Coupling	0.28~0.42
Self-inductance1	360μH
Self-inductance2	360μH
Primary additional coil *Lp*	67μH
Secondary additional coil *Ls*	67μH
Switching frequency	85 kHz
Maximum power	8 .5kW
Minimum power	4.25kW

II. The dual-sided LCC compensated wireless charger's interoperability should be evaluated under certain assumptions.

- WPT with distinct topologies are developed to interoperate by dual-side LCC compensated WPT charger constructed. Fig. 2.2 shows corresponding circuit models for the four different inter-operation types (LCC-S, LCC-P, S-LCC, and P-LCC).
- Operating frequency (ω0) is fixed, and they have same input voltage range (Vin = 0~425V), battery voltage range (Vb = 300~450V), maximum output power (Pout = 8.5kW), and misalignment tolerance (i.e., coupling coefficient range, k=3) when they interact. There is no consideration for coil design. In fact, distinct mutual inductances M can achieved by keeping similar coefficient of coupling k[4] when a coil structure is comparable.

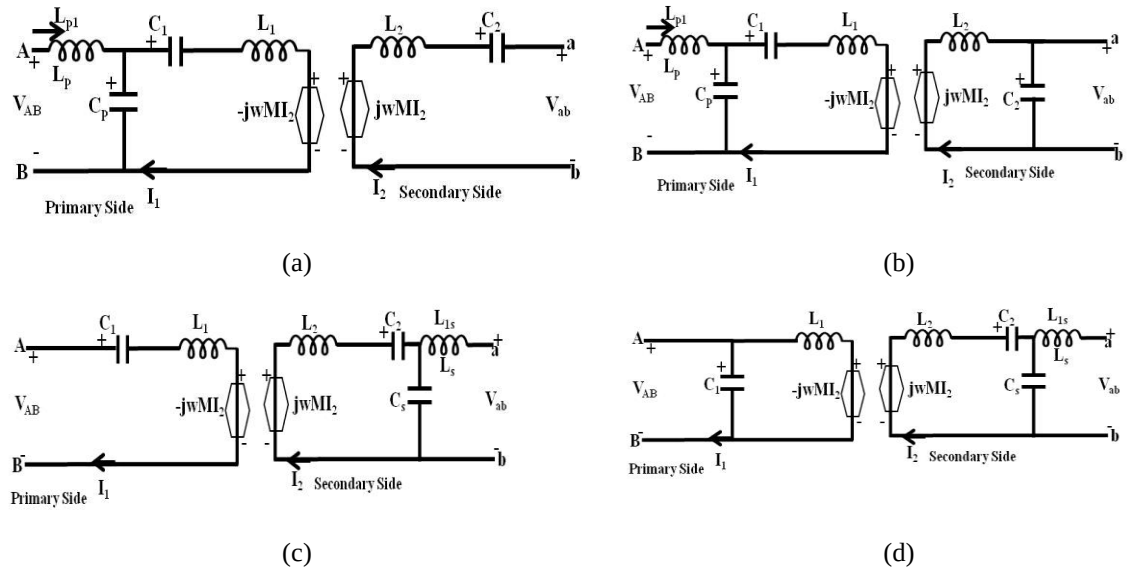

Figure 2.2: Various compensation topologies: S-LCC, P-LCC, LCC-S, and LCC-P

a). Inductance-Capacitance-Capacitance-Series Compensation Network

LCC-S interoperable depicted in Figure 2.2 (a). Under ω0 operating frequency, the input voltage VAB is the only factor affecting the primary coil 1 is constant current. A steady-state voltage source can therefore be conceptualized as the series compensated secondary side. With a steady voltage source, power transmission capacity can be infinite. Voltage following rectifier greater than battery voltage Vb since internal resistance of the battery, Ro, is taken into consideration.

The following equation is evident[6].

$$\operatorname{mod}\left\{ j\omega_o MI_1 \right\} = V_{ab} = \frac{1}{\sqrt{2}} \frac{4}{\pi} \left(\frac{P}{V_b} R_o + V_b \right) \qquad .....(2.8)$$

To attain same maximal output power and misalignment tolerance, LCC-S compensated system transfers maximum power Pmax when the primary and secondary coils are correctly aligned. It also transfers a particular amount of power Pmin when k is minimum[7]. Critical self-inductance of secondary coil L2s (Appendix "2" denotes secondary, while "s" denotes series compensation). calculated using…

$$L_{2s} = \frac{L_p^{\,2}}{k_{\min}^{\,2} L_1} \frac{V_{ab\max}^{\,2}}{V_{\mathrm{AB}\max}^{\,2}} \qquad .....(2.9)$$

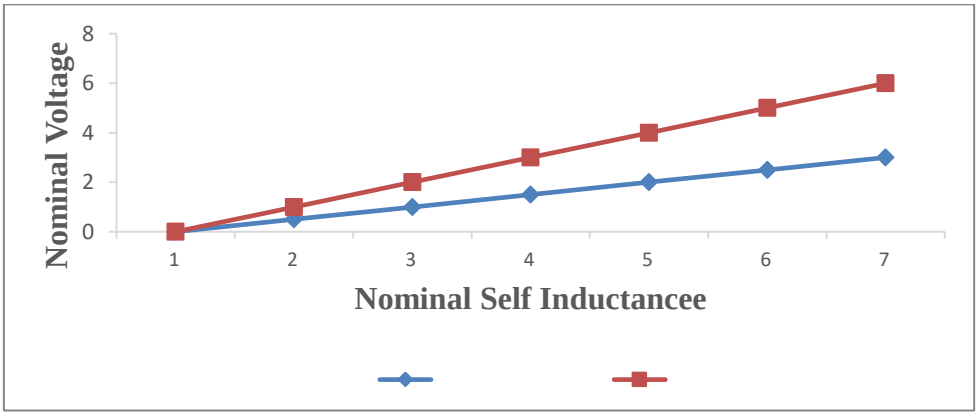

Figure 2.3: The correlation between the secondary coil's normalized self-inductance at varying coupling coefficients and the battery's maximum normalized voltage.

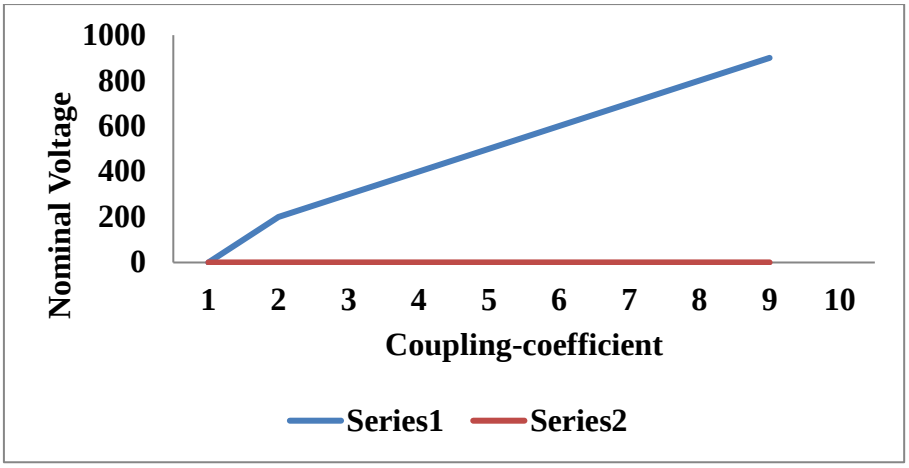

Figure 2.4: Depicts maximum battery voltage and k at various secondary coil self-inductances.

$$L_{2s} = \frac{L_p^{\,2}}{k_{\min}^{\,2} L_1} \frac{V_{ab\max}^{\,2}}{V_{AB\max}^{\,2}} \qquad \text{.....(2.10)}$$

Secondary side series capacitor can be

$$C_{2s} = \frac{1}{(\omega_0 L_{2s})}$$

…..(2.11)

Actually, input voltage VAB adjusted and produce particular desired power if the self-inductance L2>L2s on an exist series compensated secondary side[11]. Even so input current I_P will limit this. When coupling coefficient is (k_{max}), maximal output voltage can achieved, but it cannot be achieved when the coupling coefficient is (k_{min}). When coupling coefficient is k_{min}, maximum output voltage V_{ab} will be square times the value that is supposed to be. Fig. 2.5 makes this clear by showing how the self-inductance of the normalized secondary coil affects the maximum output voltage normalized. The coupling coefficient and highest possible battery voltage that can be charged when secondary coil's self-inductance is distinct are related. When k is less than 0.3, interoperable wireless charger cannot output 480V if secondary coil's self-inductance L_2 is less than critical self-inductance L_{2s}.

b). Inductance-Capacitance-Capacitance- Parallel Compensation network

Since the main coil's current is constant, as shown by following equation, LCC-P from Figure 2.2(b), the parallel secondary side as a constant current source.

$$I_o = \frac{M}{L_2} I_1$$

.....(2.12)

Appendix "2" denotes secondary, and "p" denotes parallel compensation, evaluation of LCC-S inter-operation, secondary coil critical inductance L2p acquired maximum output power (P_{max}) whenever kmax and precise quantity of output power (P_{min}) whenever kmin, consequently to (2.13) secondary coil critical inductance L_{2p} (appendix “2” means secondary, “p” means parallel compensation[9].

$$L_{2p} = \frac{k_{\max}^{\,2} L_1}{\omega_0 L_p^{\,2}} \qquad \text{.....(2.13)}$$

Relationship between normalized maximum intended power and normalized self-inductance of the receiver coil is shown in Figure 2.5 when coupling coefficient is distinct. If self-inductance of an existing parallel compensated receiver side is L_2,L_{2p}, the output power will be greater than P_{max} when V_{AB}, V_{ab}, and k are maximal. For a particular maximal output power P_{max}, we can lower the input voltage V_{AB}. If L_2>L_{2p}, output power will be square-

root times expected importance. There is one disadvantage to be aware of. Real and reactive loads were reflected back into the power supply for a receiver side that was parallelly compensated[7]. Unless frequency control is used, this topology will not achieve unity power factor.

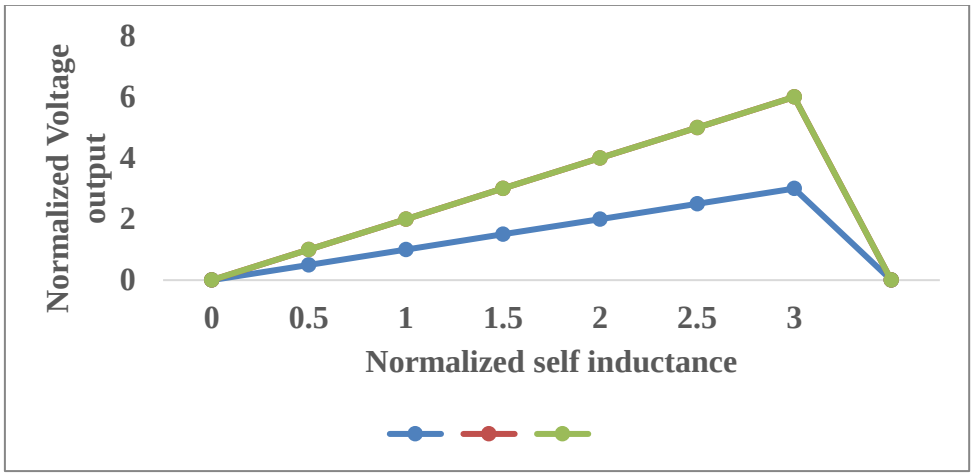

Figure 2.5: Secondary coil's normalized self-inductance at various coupling coefficients relates to its normalized maximum

output power.

c). Series-Inductance-Capacitance-Capacitance Compensation network

Figure 2.2(c) depicts circuit for S-LCC type interoperable. Because current on secondary coil I_2 is only relates to output voltage V_{ab} when operating frequency ω0, it might be thought of voltage source charging battery with a voltage of $-j\omega 0MI_2$ on primary side. Although output power capability of a constant voltage source is theoretically infinite, input voltage somewhat higher than analogous battery voltage due to the equivalent circuit's internal resistance[14]. $\mathrm{mod}\{V_{AB}\} > \mathrm{mod}\{-j\omega_0 MI_2\}$ can be obtained by ignoring the internal resistance.

In an SS WPT topology, compatibility between the series main side and the LCC secondary side. On the primary side of the SP architecture, however, the objective of the series capacitor is zero phase angle (ZPA) at a specific k[13]. SP compensated wireless charger with LCC compensated secondary side will have a higher VA rating with series compensated primary side.

d). Parallel-Inductance-Capacitance-Capacitance Compensation network

The primary parallel corrected capacitor in parallel compensated primary topologies (PS and PP topologies) is affected by the load and the coupling coefficient, as shown in Fig. 2.2(d). Consequently, applications having a fixed coupling coefficient and transferred power amount frequently employ these topologies[9]. The load varies during charging, and the coupling coefficient varies each time when a driver parks an automobile. Parallel compensated primary side is intended a fixed frequency PS or PP charger, it can be challenging for an LCC secondary side to interact [7].

III. RESULTS AND DISCUSSIONS

The electrical parameters are evaluated and their validity is verified by development and analysis of simulation models in MATLAB/SIMULINK. Consideration is given to simulating the schematic diagram in Fig. 2. The switches, transmitter, receiver, and capacitors are all under electrical stress, seen in below figures. The voltage stress on the transmitter side capacitance and transmitter coil is much higher than the inverter output voltage, as seen in Fig. 3.2. A soft switching technique is used on the inverter switches, and the zero-voltage switching (ZVS) point is depicted in Fig. 3.3. Additionally, it can be observed that the inverter switches are under current stress due to the entire transmitter current running through them. Figure 3.2. shows that electrical stress on receiver lower than transmitter side. From Fig. 3.3, it is observed load voltage and current are matched appropriate ratings of the EV battery.

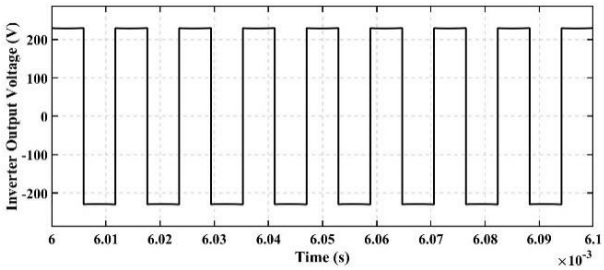

(a) voltage output of an inverter.

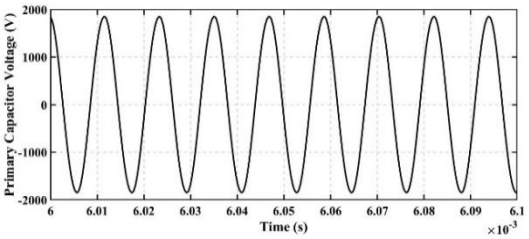

(b) voltage of the primary capacitor.

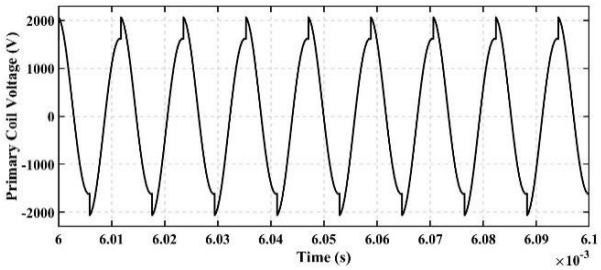

(c) voltage of the primary coil.

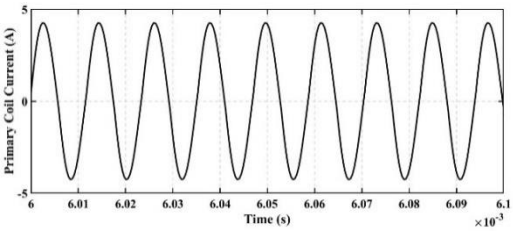

(d) current in the primary coil.

Fig 3.1: Inductive Power Transmission for Voltage Fed Topology using Transmitter Coil

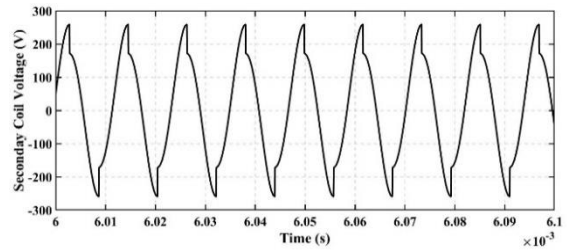

(a) Secondary coil voltage.

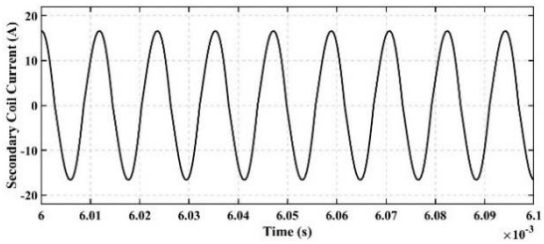

(b) Secondary coil current.

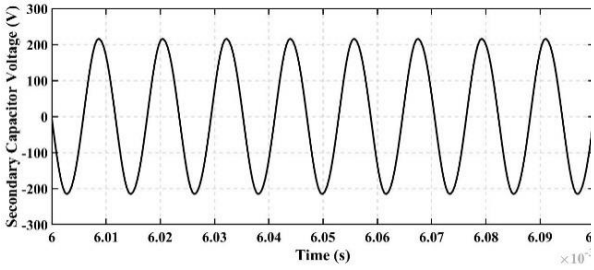

(c) voltage of the secondary capacitor.

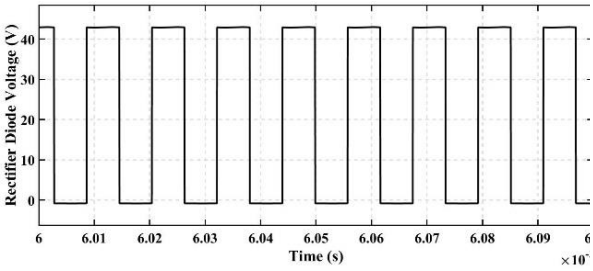

(d) voltage of rectifier diodes.

Figure 3.2: Inductive power transmission using receiver coils for voltage-fed topology.

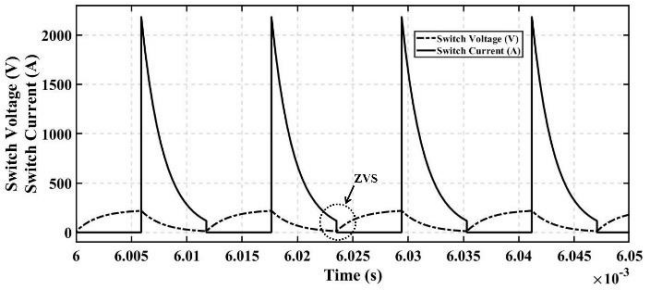

(a)

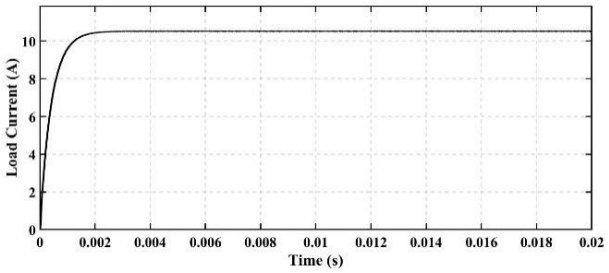

(b) Load Current.

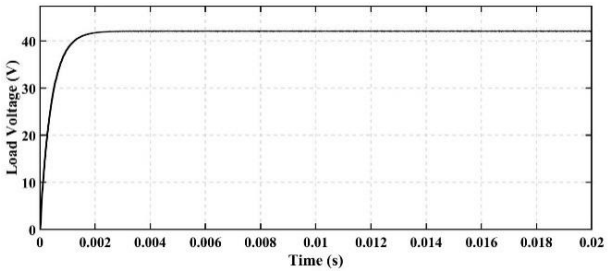

(c) Load Voltage.

Figure 3.3: S-LCC Compensation network (a)ZVS switching topology (b) Load Current for Voltage fed (c) Load Voltage

a). MATLAB Simulation Results of Dual side LCC

Dual side LCC compensated IPT system was created in MATLAB simulation to evaluate the designed dual side LCC system. Figs. 3.4–3.6 display the results of the simulation**.** The MI is considered from the FEM simulation at 265 mm vertical distance and perfect alignment of the coupled coils. Due to the presence of an additional inductor, the output current in dual side LCC compensation is lower than in SS compensation. hence power loss will present due to the additional inductor.

Thus, saw that electrical components needed to calculate mutual inductance value and obtain its performance characteristics could be obtained from current-fed compensation. The inverter device voltage is higher, the primary capacitor depends on the load and coupling factor, the current-fed configuration avoids instantaneous voltage changes, and the main benefits of the impedance transferred are high efficiency, high power factor at relatively low mutual inductance, and a large range of load variation, but power factor is not at unity.

The performance of the transmitter coil for inductive power transmission is displayed in Fig. 3.4, and evaluated parameters are simulated in MATLAB/SIMULINK. Fig. 3.5 displays the receiver coil's performance for the transmission of inductive power. In Fig. 3.6, load voltage and load current are displayed.

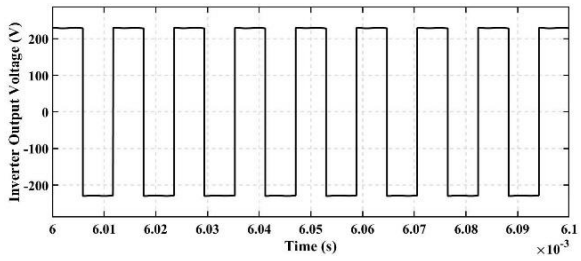

(a) Inverter output voltage.

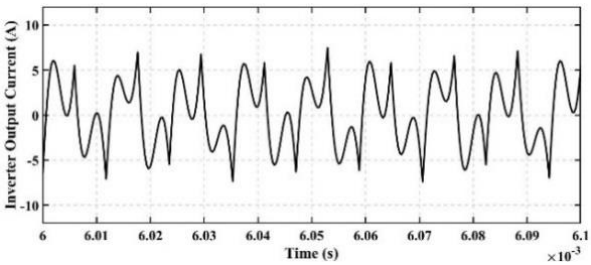

(b) Inverter output current.

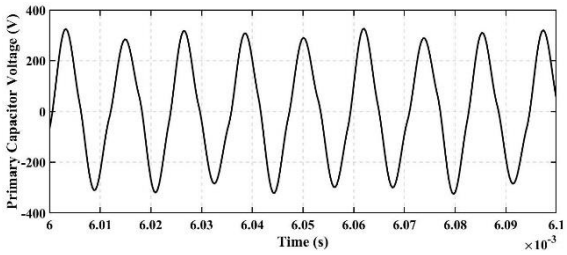

(c) Primary capacitor voltage.

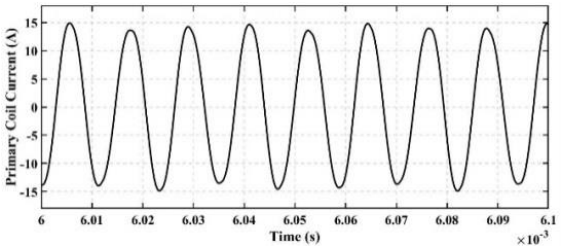

(d) current in the primary coil.

Figure 3.4 implementation of current-fed topology for transmitter coil inductive power transmission.

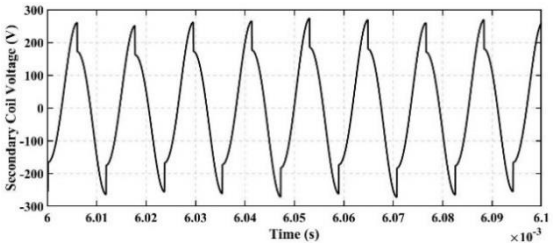

(a) Secondary coil voltage.

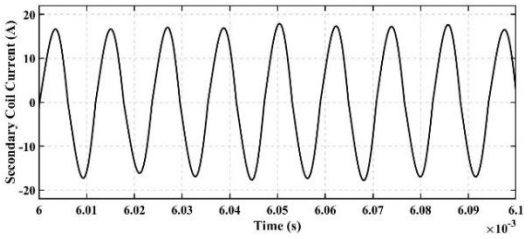

(b) Secondary coil current.

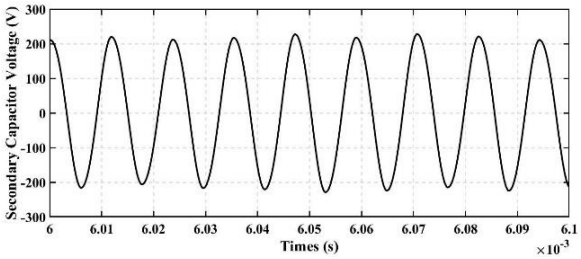

(c) voltage of the secondary capacitor.

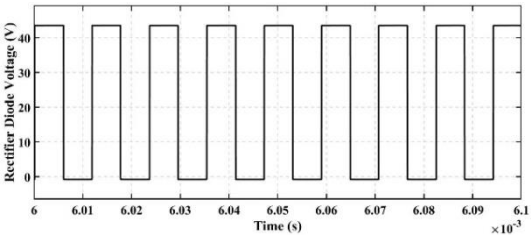

(d) voltage of rectifier diode.

Figure 3.5 : Implementation of current fed architecture for receiver coil inductive power transmission.

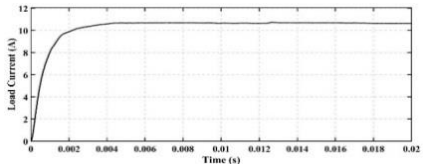

(a) Load Current.

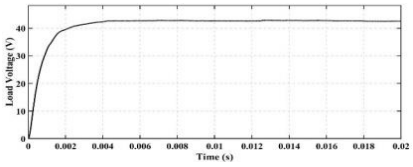

(b) Load Voltage

Figure 3.6 : Voltage and Current of the Load

Table I displays the parameters that were evaluated for inductive power transmission. Same parameters for both the voltage-fed and current-fed topologies are used for simulation model and analysis. The characteristics that are compared between the inductive power transfer topologies and are displayed in Table-II include source protection, coil weight, inverter switches voltage stress, transmitter side capacitor current stress, and transmitting coil voltage stress.

Table-II: Parameters of Voltage-Fed and Current-Fed Topologies

Parameters	**Values**
Output Voltage, (V_0)	48V
Output Current, (I_0)	12A
Source Votage, ($V_{s,rms}$)	44V

Parameters	**Values**
Source Current, ($I_{s,rms}$)	15A
Inverter Votage, ($V_{peak, rms}$)	230V
Load Resistance, (R_0)	10Ω
Input Inductance, (L_d)	56μH
Primary Inductance, (L_p)	39μH
Secondary Inductance, (L_s)	28μH
Mutual Inductance, (M)	7.6μH
Primary Capacitance, (C_p)	100nF
Secondary Capacitance, (C_s)	150nF

Table-III: Qualitative Comparison of Inductive Power Transfer Topologies

Features	**Voltage-fed Topology**	**Current-fed Topology**
Transmitter side capacitor voltage stress	Maximum	Medium
Transmitting coil Voltage stress	Maximum	Medium
Transmitter side capacitor current stress	Medium	Maximum
Inverter switches voltage stress	Medium	Medium
Source protection	Unsafe	Safe
Coil weight	High	Less

IV. CONCLUSION

The compatibility of wireless chargers manufactured by various firms is a commonly expressed concern. This chapter discusses the interoperability of several compensation topologies. Interoperability considerations between various topologies constitute the main focus of this chapter. Reference wireless charger is a dual-sided LCC wireless charger. A detailed discussion of design concerns is given to the four types of inter-operations: LCC-S, LCC-P, S-LCC, and P-LCC. A double-sided LCC compensatory topology wireless charger was redesigned as an LCC-S type wireless charger in order to test the analysis. Efficiency of current-fed converter topologies DC - DC is 95.8%. A detailed comparison of the features and results of both topologies shows that the current-fed topology performs better for inductive wireless power transmission in terms of coil weight, source protection, voltage stress on the inverter being within limits, and low voltage stress on the transmitted side. Even at a 300mm gap, there is a 265mm misalignment. For resonant IPT system performance analysis, dual side LCC compensation topologies are described and compared. In general, electrical characteristics of these compensation topologies are influenced by changes in mutual inductance (misalignments). The voltage and current stress on the elements of dual side LCC compensation are smaller when compared to S/S compensation, according to simulated and measured analysis.

REFERENCES

1. Covic G. A. and Boys J. T. (2013) “Modern Trends in Inductive Power Transfer for Transportation Applications” IEEE Transactions Journal of Emerging and Selected Topics in Power Electronics, 1(1), 28–41.
2. C. Qiu, K. T. Chau, C. Liu, and C. C. Chan, (2013)“Overview of wireless power transfer for electric vehicle charging,” Electr. Veh. Symp. Exhib. (EVS27), 2013 World, vol. 7, April 2013, pp. 1–9.

3. M. Budhia, G. A. Covic, and J. T. Boys,(2011) “Design and optimization of circular magnetic structures for lumped inductive power transfer systems,” IEEE Trans. Power Electron., vol. 26, no. 11, pp. 3096–3108.
4. Ravi Bukya, Mangu, A.Jayaprakash and Jatoth Ramesh " A Study on Current-fed Topology for Wireless Resonant Inductive Power Transfer Battery Charging System of Electric Vehicle” PARC-2020, feb-28-29,vol.1,pp May-2020.
5. C. S. Wang, O. H. Stielau, and G. A. Covic, “Design consideration for a contactless electric vehicle battery charger,” IEEE Trans. Ind. Electron., vol. 52, No. 5, pp. 1308–1313, Oct.2005.
6. G. Ombach, “Design and Safety Considerations of Interoperable Wireless Charging System for Automotive,” Ninth International Conference on Ecological Vehicles and Renewable Energies, EVER 2014, 25-27 March 2014, pp.1-4.
7. A.P. Sample, D.A. Meyer and J.R. Smith, “Analysis, experimental results, and range adaptation of magnetically coupled resonators for wireless power transfer,” IEEE Trans. Industrial Electronics, vol. 58, No. 2, pp. 544-554, Feb. 2011.
8. Y. Guo and Y. Zhang, "Secondary Side Voltage and Current Estimation of Wireless Power Transfer Systems," in IEEE Transactions on Industry Applications, vol. 58, no. 1, pp. 1222-1230, Jan.-Feb. 2022, doi: 10.1109/TIA.2021.3092311.
9. B. Mangu, S. Akshatha, D. Suryanarayana and B. G. Fernandes, “Grid-Connected PVWind-Battery based Multi-Input Transformer Coupled Bidirectional DC-DC Converter for household Applications,” IEEE Trans. Emerg. Sel. Topics Power Electron., vol. 4, no.3, Sept. 2016.
10. Y. Yorozu, M. Hirano, K. Oka, and Y. Tagawa, “Electron spectroscopy studies on magneto-optical media and plastic substrate interfaces(Translation Journals style),” IEEE Transl. J. Magn.Jpn., vol. 2, Aug. 1987, pp. 740–741 [Dig. 9th Annu. Conf. Magnetics Japan, 1982, p. 301].
11. Pradipta Patra, Susovon Samanta, Amit Patra, Souvik Chattopadhyay, “A Novel Control Technique for Single-Inductor Multiple-Output DC-DC Buck Converters”, IEEE International Conference on Industrial Technology, Mumbai, India, 15-17 Dec. 2006.
12. S. Samanta, A.K. Rathore, Sanjib Kumar Sahoo, “Current-fed full-bridge and half-bridge topologies with CCL transmitter and LC receiver tanks for wireless inductive power transfer application”, IEEE Region 10 Conference (TENCON), Singapore, 22-25 Nov. 2016.
13. V.R. kiran, R.K Keshri, Manuele Bertoluzzo, “Efficient Wireless Charging of Batteries With Controlled Temperature and Asymmetrical Coil Coupling” IEEE International Conference on Power Electronics, Drives and Energy Systems (PEDES), Chennai, India, 18-21 Dec. 2018.
14. Y. Guo; Y Zhang, B. Yan, Ke Wang, Z Zhang, Lifang Wang "Interoperability Analysis of Compensation Network in Electric Vehicle Wireless Charging System" 2018 IEEE International Power Electronics and Application Conference and Exposition (PEAC), Shenzhen, China, 27 December 2018.
15. J. Dai and D. C. Ludois, “A survey of wireless power transfer and a critical comparison of inductive and capacitive coupling for small gap applications,” IEEE Trans. Power Electron., vol. 30, no. 11, pp. 6017–6029, 2015.
16. T. Kan, F. Lu, T.-D. Nguyen, P. P. Mercier, and C. C. Mi, “Integrated coil design for EV wireless charging systems using LCC compensation topology,” IEEE Trans. Power Electron., vol. 33, no. 11, pp. 9231–9241, 2018.
17. S. R. Hui and W. W. Ho, “A new generation of universal contactless battery charging platform for portable consumer electronic equipment,” IEEE Trans. Power Electron., vol. 20, no. 3, pp. 620–627, 2005.
18. J. T. Boys and G. A. Covic, “The inductive power transfer story at the University of Auckland,” IEEE Circuits Syst. Mag., vol. 15, no. 2, pp. 6–27, 2015.

AUTHORS PROFILE

Bhaskar Bhookya received his BTech in Electrical and Electronics Engineering from JNTUH(VIFCET), Hyderabad, India, in 2008, MTech from the JNTUH(REC) in 2011. Currently, he is pursuing his PhD research work in the Department of Electrical and Electronics Engineering at the UCE,OU, Hyderabad. His areas of Research interests are DC-DC Current-fed Converter, Electric Drives, Electric Vehicle Charging System, Wireless charging system, microgrid control and parallel operation of inverters in microgrid.

Prof. B Mangu received his Ph.D from the Indian Institute of Technology Bombay, Mumbai, India, in 2016. He is working as an Professor in the Department of Electrical Engineering, University College of Engineering, Osmania University, India. He has published many articles in international journals/conferences and is a senior member of the IEEE and Fellow of Institute of Engineer. His main research interests are in the areas of Power Electronics Converter for Renewable Energy, DG, power electronics, and Wireless Power Transfer for Electric Vehicle.

Dr. Ravi Bukya completed his Phd in Electrical Engineering from university college of engineering, Osmania university in 2023, received his BTech in Electrical and Electronics Engineering from Nethaji Institute of Engineering and Technology, (NIET), Hyderabad, India, in 2009, MTech from the JNTUH(DARECET) in 2013.His areas of research interests are DC-DC Current-fed Converter, Electric Vehicle Charging System, Wireless charging system.